# Supplementary Information

## Experimental details

***Materials and chemicals:***

Lithium bis((trifluoromethyl)sulfonyl)azanide (LiTFSI) were purchased from Sigma-Aldrich. Tetraethylene glycol dimethyl ether (TEGDME) and dimethyl sulfoxide (DMSO) were purchased from Macklin. Super P carbon (SP) and polytetrafluoroethylene (PTFE) was purchased from Dodochem. The quartz crystal electrode was purchased from CH Instruments. Its thickness is 0.21 mm, its area is 0.22 $cm^2$, and its resonant frequency is 7.995 MHz. Before use, LiTFSI was vacuum-dried at 120°C for 24 hours, and TEGDME and DMSO were dehydrated using 4 Å molecular sieves. All materials were stored in an argon-filled glove box with a moisture content of less than 0.1 ppm. No further purification of the materials was performed before use. The electrolyte used in this study is 1 M LiTFSI in TEGDME/DMSO.

***Characterization:***

The morphology of the products was observed using a scanning electron microscope (SEM, JEOL S-4800). The types of discharge products were characterized using Raman spectroscopy (Raman, Horiba XploRA Plus). The yield of $Li_2O_2$ was quantified using ultraviolet-visible spectroscopy (UV-vis, SDPTOP-756PC). The vibrating frequency of the crystal electrode was in situ recorded using the quartz crystal microbalance (QCM) function of an electrochemical workstation (CHI 440)[1, 2].

***Electrochemical testing:***

The electrochemical deposition-dissolution experiments were conducted using a custom-made QCM mold, as shown in Figure 1a. During the electrochemical testing, the QCM functionality was used simultaneously. Perform cyclic voltammetry (CV) on the crystal electrode in a 10 mM $AgNO_3$ and 0.1 M $KNO_3$ aqueous solution with a scan rate of 10 mV $s^{-1}$. Simultaneously use the QCM functionality of the electrochemical workstation to establish the relationship between the vibration frequency and mass of the crystal electrode.

$Li_2O_2$ deposition experiments: The deposition of $Li_2O_2$ on the crystal electrode was achieved by performing linear sweep voltammetry (LSV) in the $O_2$-saturated electrolyte with a scan rate of 2 mV $s^{-1}$. The electrolyte used was 1 M LiTFSI in TEGDME. For experiments at different angles, the electrode was positioned at 0°, 45°, 90°, and 135° in the electrolyte. A custom-made QCM mold enabled testing at these different angles. The working electrode, reference electrode, and counter electrode were quartz crystal electrode (Au), Ag/AgCl electrode, and Li foil, respectively. The effects of different electrode materials were studied by replacing the working electrode with Pt or C crystal electrodes.

$Li_2O_2$ dissolution experiments: To measure the dissolution rate of $Li_2O_2$, we removed the discharge current after the deposition process and recorded the mass change of the electrode surface using QCM functionality. When measuring the intrinsic dissolution rate of $Li_2O_2$, we applied a small reduction current (2 nA, eq. 9 nA $cm^{-2}$, two orders of magnitude smaller than the actual discharge current) to maintain the discharge state of the electrode surface and the adsorption state of the $Li_2O_2$, while recording the mass change of the electrode surface. A tiny discharge current of 2 nA is equivalent to $Li_2O_2$ depositing rate of 0.12 ng $cm^{-2}$ $min^{-1}$, two orders of magnitude smaller than the dissolving rate. To study the effect of the solvent on the dissolution process, we replaced the electrolyte with 1 M LiTFSI in DMSO and used the same testing method.

The discharge experiments with vertical and upward electrodes were conducted in the same $O_2$-saturated electrolyte. The electrolyte was 1 M LiTFSI in TEGDME. The working electrode, reference electrode, and counter

electrode were Au plate electrode (at 0° and 90°), Ag/AgCl electrode, and Li foil, respectively. The testing conditions involved constant current discharge at a current density of 1.5 and 3 μA $cm^{-2}$.

The intermittent discharge experiments were conducted in a lithium-oxygen mold cell. The positive electrode was a porous electrode exposed to $O_2$. The porous electrode was made by uniformly mixing SP and PTFE in a 4:1 ratio and coating it onto carbon paper. The active material loading was approximately 3 mg $cm^{-2}$. The negative electrode was Li. The electrolyte was 1 M LiTFSI in TEGDME. The Glass Fiber GF/F was used as separator. The intermittent discharge involved discharging the cell at a constant current density of 0.22 mA $cm^{-2}$ for 10 minutes, then stopping, and holding the cell voltage at 2.9 V for 3 minutes before repeating the cycle. The control group involved continuous discharge of the cell at a constant current density of 0.22 mA $cm^{-2}$ until the cut-off voltage was reached.

Calculation of the $Li_2O_2$ thickness on Au-90°:

$$H = \frac{m}{S \cdot \rho}$$

In this context, H represents the thickness of $Li_2O_2$ (cm), m denotes the mass of $Li_2O_2$ (g), ρ signifies the density of $Li_2O_2$ (g $cm^{-3}$), and S indicates the electrode area ($cm^2$). The calculations in the text use a density of 1.2 g $cm^{-3}$ and an electrode area of 0.22 $cm^2$.

***Calculation of the $Li_2O_2$ yield:***

The yield of $Li_2O_2$ is quantified using UV-Vis spectroscopy. The $Li_2O_2$ forms a pale yellow complex $[Ti(O_2)]^{2+}$ in the titration solution (2% $TiOSO_4$ dissolved in 1 M $H_2SO_4$). This complex has an absorption peak at $\lambda_{max}$ = 405 nm. The intensity of this absorption peak can be used to calculate the content of $Li_2O_2$[3]. By directly adding a known quantity of $Li_2O_2$ to the titration solution, an absorbance of A=1 is obtained at $\lambda_{max}$ = 405 nm for a discharge amount of 0.225 mAh. Therefore, with a known discharge capacity, the yield of $Li_2O_2$ can be determined by diluting the $Li_2O_2$ on the electrode to the same extent and measuring the absorbance at $\lambda_{max}$ = 405 nm. A trace amount of $Li_2O_2$ was titrated using N, N-diethyl-1,4-phenylenediamine (DPD). The samples were placed in tubes containing 0.4 mL buffer solution, 3 mL $H_2O$, 0.05 mL DPD, and 0.05 mL hydrogen peroxidase, and the resulting solution was tested by UV-Vis spectroscopy. The buffer solution was prepared by mixing 1 M potassium dihydrogen phosphate and 1 M dipotassium phosphate in a volume ratio of 7:1. The yield of $Li_2CO_3$ was quantified using DEMS. An excess of phosphoric acid was added to the sample, and the $CO_2$ produced during the reaction was detected by DEMS.

***Estimating the Charging Current:***

$$\text{Charging Current} = \frac{\text{actual dissolution rate} \times F}{M_{Li_2O_2}}$$

$$\text{actual dissolution rate} = \text{measured dissolution rate} \times \text{effective exposure area}$$

$$\text{effective exposure area} = \frac{\frac{Q \times M_{Li_2O_2}}{F}}{m_{Li_2O_2\text{ - torus}}} \times S_{Li_2O_2\text{ - torus}} \times \text{effective coefficient}$$

$$m_{Li_2O_2\text{ - torus}} = \rho_{Li_2O_2} \times V_{Li_2O_2\text{ - torus}}$$

$$V_{Li_2O_2\text{ - torus}} = \frac{1}{4}\pi^2 r_{Li_2O_2}^3$$

## Supplementary Figures

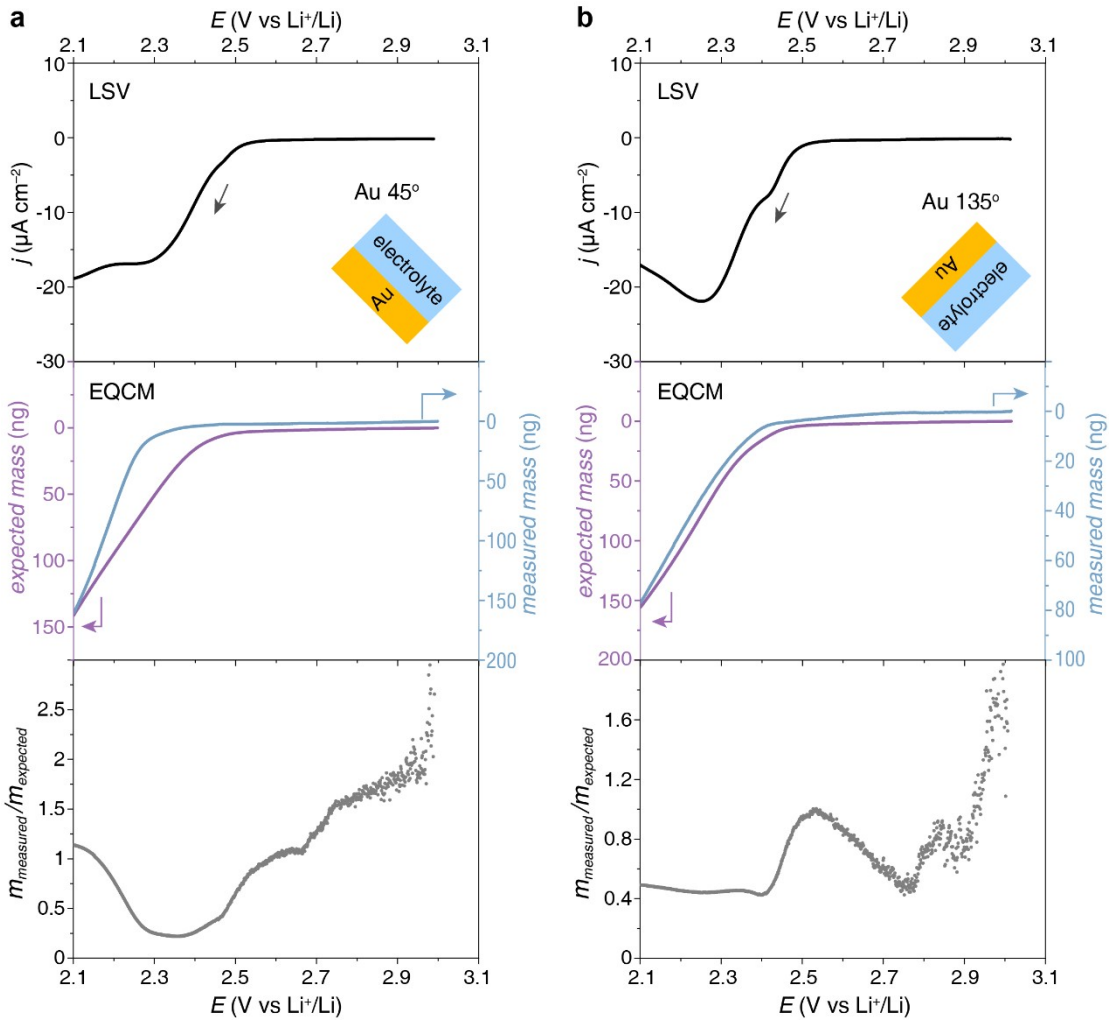


**Figure S1.** The deposition results on the Au crystal electrode at 45° and 135°.

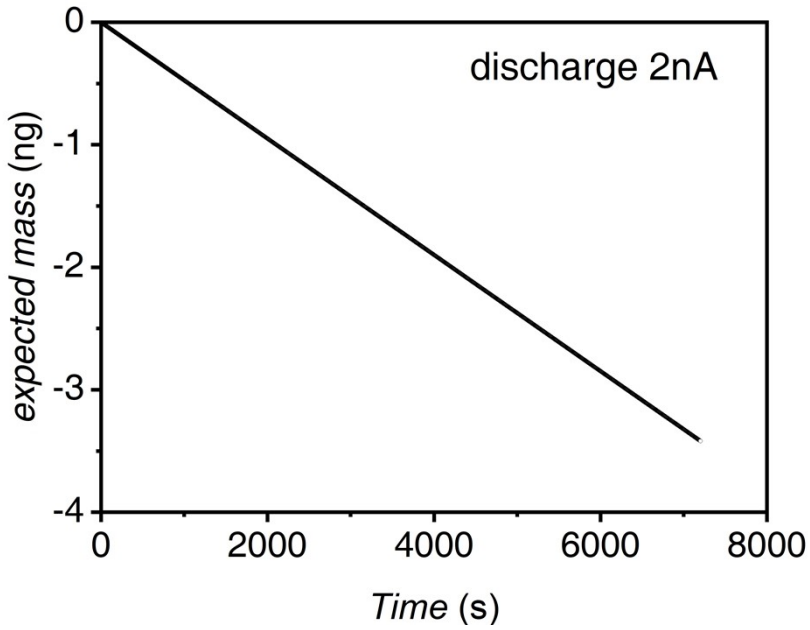


**Figure S2.** The product deposition rate corresponding to the 2 nA reduction current is 0.12 ng $cm^{-2}$ $min^{-1}$. The amount of $Li_2O_2$ generated in this electrochemical process is much lower than the amount of $Li_2O_2$ dissolved from the electrode surface, so it can be neglected.

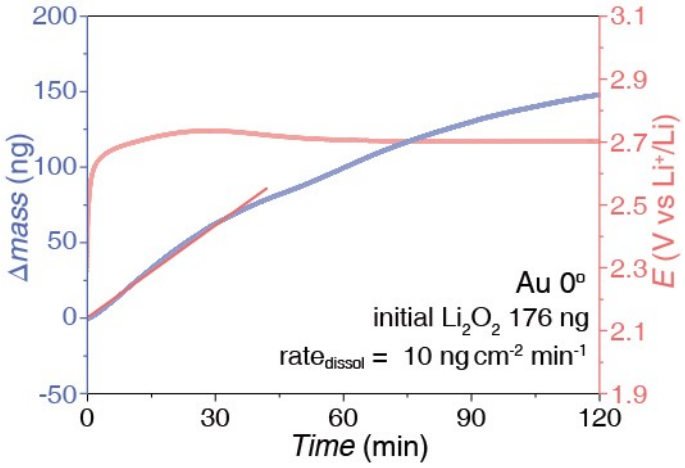


**Figure S3.** The dissolution rate of products on the electrode (Au-0°) with 2 nA reduction current applied, when the initial $Li_2O_2$ amount was 176 ng. It demonstrates that the initial amount of products on the electrode surface does not affect the dissolution rate.

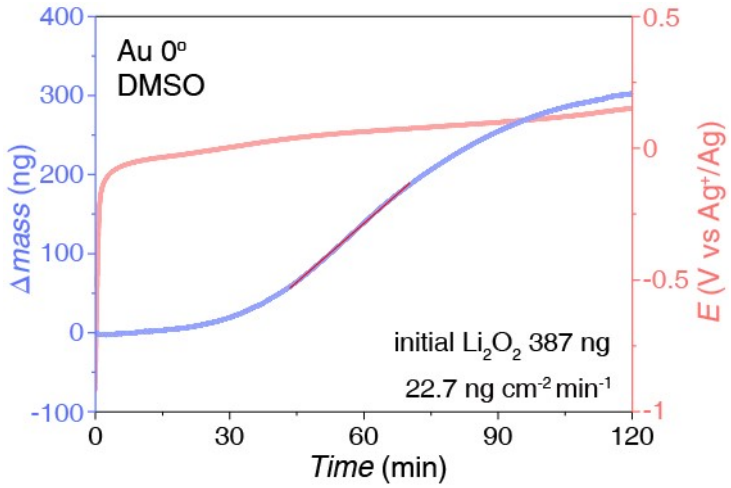


**Figure S4.** The dissolution rate of products on the Au electrode (Au-0°) surface in DMSO-based electrolyte. The initial $Li_2O_2$ amount was 387 ng.

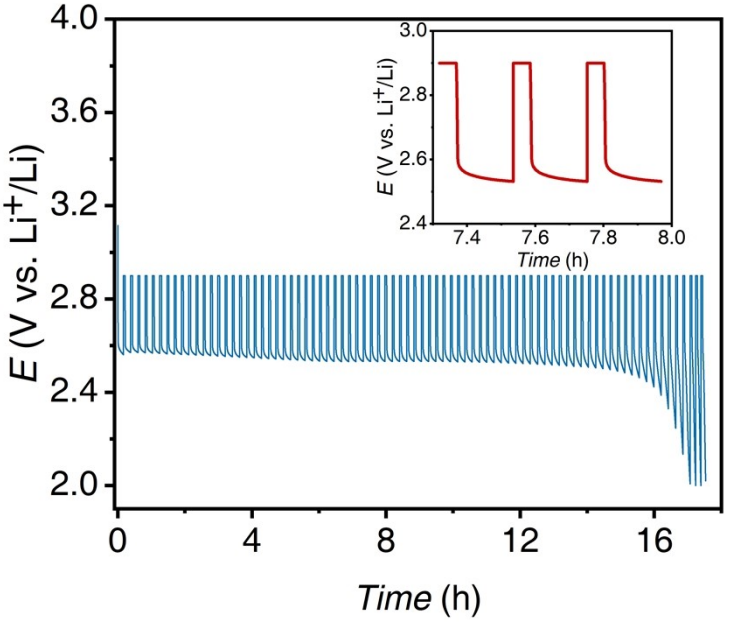


**Figure S5.** Discharge curves of intermittent-desorption discharge lithium-oxygen battery. Current density: 0.22 mA $cm^{-2}$.

## References


1. Y. Ji, Z.-W. Yin, Z. Yang, Y.-P. Deng, H. Chen, C. Lin, L. Yang, K. Yang, M. Zhang, Q. Xiao, J.-T. Li, Z. Chen, S.-G. Sun and F. Pan, *Chem. Soc. Rev.*, 2021, **50**, 10743-10763.
2. G. Vanhoutte, S. Schaltin, M. Wu, F. Bardé and J. Fransaer, *ECS Meeting Abstracts*, 2015, **MA2015-03**, 454.
3. Y. J. Lee, W.-J. Kwak, Y.-K. Sun and Y. J. Lee, *ACS Appl. Mater. Interfaces*, 2018, **10**, 526-533.